# Technical note: Assessing pretreatment approaches for serial pyrolysis-oxidation analysis of sedimentary organic carbon

Songfan He<sup>1</sup>, Huiyuan Yang<sup>1</sup>, Xingqian Cui<sup>1</sup>

<sup>1</sup>School of Oceanography, Shanghai Jiao Tong University, Shanghai, 200030, China Correspondence to: Xingqian Cui (cuixingqian@sjtu.edu.cn) or Huiyuan Yang (yhy 0707@sjtu.edu.cn)

**Abstract.** The ramped-temperature pyrolysis/oxidation (RPO) analysis has emerged as a powerful analytical technique for characterizing sedimentary organic carbon (OC), bridging the knowledge gap between bulk carbon and molecular-level analyses. While acid pretreatment is routinely employed to remove carbonates prior to RPO analysis, its methodological impacts remain poorly constrained compared to other geochemical measurements (e.g.,  $\delta^{13}$ C). Given the widespread utilization of RPO analysis in recent studies, a comparative examination of pretreatment conditions is timely to ensure unbiased acquisition of thermochemical results. This study systematically evaluates how decarbonation protocols influence RPO results through comparative analyses of different pretreatment approaches. We demonstrate that both acidification method (rinsing *vs.* fumigation) and HCl concentration significantly affect RPO thermograms, with observed differences attributed to the alteration of organic-inorganic associations and selective leaching of acid-soluble OC. Notably, results from diluted acid rinsing are more similar to the raw material. Based on comprehensive testing, we recommend diluted HCl rinsing with moderate reaction times (~ 12h) as the optimal pretreatment for most samples, while acknowledging that specific sample characteristics (e.g., organic lean, protein rich) may necessitate adjustments to the protocol. These finding highlight the importance of pretreatment conditions in thermochemical decomposition studies.

#### 20 1 Introduction

Organic geochemical proxies serve as powerful tools for reconstructing natural processes across modern and ancient environments. Current approaches primarily utilize either bulk analyses (e.g., organic carbon contents,  $\delta^{13}C_{org}$ ) that provide integrated sample information, or molecular biomarkers (e.g., fatty acids, sterols) that offer source-specific insights. Bridging these scales, the ramped-temperature pyrolysis/oxidation (RPO) technique has emerged as a transformative approach that interprets organic carbon (OC) as a thermal reactivity continuum, effectively deconvoluting bulk signatures into component fractions (Cui et al., 2022; Hemingway et al., 2017a; Rosenheim et al., 2008). The RPO analysis progressively converts OC to  $CO_2$  across a temperature gradient, with thermochemically labile OC being decomposed at lower temperatures and refractory OC at higher temperatures. Thus, OC of different sources (e.g., biogenic OC, rock-derived OC) and thermochemical behaviors can be, in part, discriminated in RPO analyses. This offers a window to "unfold" bulk C data to two-dimensional configurations

characterized by OC species with relative quantities. This capability has significantly advanced studies of sediment chronology (Rosenheim et al., 2008, 2013; Venturelli et al., 2020), regional OC dynamics (Bao et al., 2018; Hemingway et al., 2018; Maier et al., 2025; Zhang et al., 2017; Zhang et al., 2022), and global organo-mineral interactions (Cui et al., 2022; Hemingway et al., 2019).

Generally, the removal of inorganic carbon through decarbonation represents a critical pretreatment step for RPO analysis of sedimentary OC. Currently, decarbonation approaches include two different methods. Acid rinsing involves direct addition of hydrochloric acid (HCl) solution to particulates in the aqueous phase followed by subsequent rinses with Milli-Q water, while acid fumigation features direct exposure of particulates to HCl acid in the vaporous phase (Harris et al., 2001). Moreover, acid rinsing may vary in concentrations of HCl being applied (Kim et al., 2016; Pasquier et al., 2018), while acid fumigation in some cases is followed by water rinsing to remove chlorides (Hemingway et al., 2017a). These various acidification pretreatments can yield diverse impacts on OC compositions (Brodie et al., 2011; Komada et al., 2008; Lohse et al., 2000; Schlacher and Connolly, 2014). Specifically, acid rinsing can potentially result in OC dissolution/hydrolysis (Fujisaki et al., 2022; Galy et al., 2007; Serrano et al., 2023), whereas acid fumigation is thought to alter organo-mineral interactions (Plante et al., 2013) and is unsuitable for samples rich in carbonates (Hedges and Stern, 1984). Furthermore, the choice between freezedrying and oven drying introduces additional variability in OC composition (De Lecea et al., 2011; Kim et al., 2016; McClymont et al., 2007). Despite widespread examination deployed for bulk parameters, systematic evaluation of pretreatment-induced artifacts remains notably lacking for RPO analysis (Bao et al., 2019; Hemingway et al., 2019). This knowledge gap necessitates comprehensive investigation of decarbonation pretreatments given the increasing adoption of RPO technique in organic geochemistry studies.

In this study, we systematically evaluate how pretreatment conditions influence RPO results by testing a suite of variables. Variables of consideration include acidification methods (rinsing *vs.* fumigation), concentrations of hydrochloric acid (1 N, 2 N, 4 N, 6 N and 12 N for fumigation), reaction durations (6 h, 12 h and 24 h), drying methods (freeze-drying *vs.* oven drying), oven drying temperatures (45 °C *vs.* 60 °C), and acid reaction temperatures (ambient *vs.* 60 °C). Using RPO analyses supplemented with bulk measurements (TOC and δ<sup>13</sup>C<sub>org</sub>), we assess the potential alteration of chemical structures and changes in OC quantities and compositions induced by pretreatment conditions. Our results establish the protocol that minimizes artifacts while maintaining analytical integrity, providing standardized pretreatment operations for this rapidly advancing technique.

### 2 Materials and methods

### 2.1 Samples and preparation

Four samples with different properties were selected, including two lithified ancient sediments and two modern sediments.

These samples were collected, respectively, from: (i) the Eocene Green River Formation (sedimentary rock, termed "SR1");

(ii) the Permian-Triassic Meishan section (sedimentary rock, termed "SR2"); (iii) the Yangtze River Estuary (modern sediment, termed "Sed1"); and (iv) Isfjorden fjord of Svalbard (modern sediment, termed "Sed2"). Two rock samples (i.e., SR1 and SR2) have similar TOC values but contrasting carbonate contents, whereas the other two surface sediment samples (i.e., Sed1 and Sed2) are similar in carbonate contents, but are differentiated by TOC values. All these samples were grounded into powder, homogenized, and divided into 13 aliquots, respectively, for subsequent processing.

## 2.2 Experimental design and operations

65

75

90

We conducted two contrasting acidification pretreatments, i.e., acid rinsing and acid fumigation. Particularly, acid rinsing was conducted with additionally various conditions to compare the influence of HCl concentrations, acidification durations, drying methods and temperatures, the potential influence of heating at decarbonation reactions and prolonged exposure to concentrated acid. Furthermore, two sets of acid fumigation pretreatments were carried out to compare with acid rinsing and to examine the impact of water rinsing following acid fumigation (Bao et al., 2019; Harris et al., 2001; Hemingway et al., 2017a). Major variables and corresponding parameters are summarized in Table 1, while detailed conditions and results of other minor factors (e.g., reaction time and drying method) are provided in the supplementary file.

For acid rinsing, each aliquot (> 200 mg) was weighed in a 50 mL glass centrifuge tube, followed by the addition of HCl with a specific concentration (i.e., 1 N, 2 N, 4 N or 6 N). To ensure the complete removal of IC, we gradually added HCl in excess. Moreover, we stirred solid-liquid mixtures during and after acidification using a portable vortex mixer. To investigate the effect of heating, one aliquot was maintained at 60 °C (± 3 °C) for 1 h after acidification. All reactions were set for 6 h, 12 h, or 24 h according to designated experimental conditions (see Table S1). Afterwards, the supernatants were removed using pipettes after centrifugation and the residual solids were rinsed with Milli-Q water three to four times to be neutralized.

For acid fumigation, two sets of subsamples were weighed and placed in a glass petri dish ( $\Phi$  60 mm × 35 mm). Before fumigation, we carefully added several drops of Milli-Q water to moisten subsamples (Harris et al., 2001; Yamamuro and Kayanne, 1995). Eight subsamples were then placed into a bilayer glass desiccator, being exposed to a glass beaker of  $\sim$  50 mL 12 N HCl beneath at room temperature for 12 h. After fumigation, subsamples were supplied with two additional drops of aqueous HCl to verify the completeness of decarbonation. This is based on the former practice that acid fumigation is not suitable for samples containing a great portion of CaCO<sub>3</sub> (Hedges and Stern, 1984). As expected, two subsamples of SR1 containing  $\sim$  70% w/w CaCO<sub>3</sub> bubbled violently, indicating residual carbonate, whereas the others show no visible reaction. We then added HCl in excess to completely remove unreacted CaCO<sub>3</sub> in SR1 subsamples. Afterwards, one set of subsamples (SR1, SR2, Sed1, Sed2) therein were additionally rinsed with Milli-Q water for three times prior to freeze-drying.

Air drying at room temperature, oven drying and freeze-drying are typical drying methods, with the latter two being compared in this study. The majority of subsamples were freeze-dried at -60 °C for more than 24 h while two sets were dried in an oven at 45 °C or 60 °C for  $\sim$  40 h (Table S1), respectively. Two different temperatures were adopted to examine possible influence of oven drying temperatures. Fumigated subsamples were dried at 60 °C given that low temperature is inefficient in removing

water vapor since the fumigated subsamples is prone to moisture absorption. To minimize the corrosive effect of vaporized HCl, fumigation subsamples were oven dried aside with sodium hydroxide flakes. After drying, subsamples were homogenized with an agate mortar and pestle. All glass containers were pre-combusted at 550 °C for 6 h to eliminate contaminants.

**Table 1.** Combinations of main experimental conditions investigated in this study, including acidification methods, HCl concentrations, reaction durations and temperature, as well as drying methods and temperature.

Acidification method	HCl concentration	Reaction temperature	Duration	Drying method
Rinsing	1 N	Ambient	12 h	Freeze-drying
Rinsing	2 N	Ambient	12 h	Freeze-drying
Rinsing	4 N	Ambient	12 h	Freeze-drying
Rinsing	6 N	Ambient	12 h	Freeze-drying
Fumigation + Rinsing	12 N	Ambient	12 h	Freeze-drying
Fumigation	12 N	Ambient	12 h	Oven drying, 60°C

<sup>§</sup>The control group is 1 N HCl. We emphasize it is not necessarily to be the best choice of experimental condition. It is based on the experiment design and is only used to facilitate comparisons between different conditions.

#### 2.3 Bulk carbon measurement

100

105

115

Each homogenized carbonate-free subsample was divided into two aliquots for bulk and RPO analyses (see Sect. 2.4), respectively. For the bulk carbon measurement, an aliquot containing  $\sim 200~\mu g$  OC was weighed, placed and wrapped in a tin capsule. Sample-containing tin capsules were transferred into the autosampler of a Thermo Fisher Scientific Flash IRMS elemental analyzer (EA) coupled to an Electron DELTA V Advantage isotope ratio mass spectrometer (IRMS). The resulting TOC and  $\delta^{13}C_{org}$  values (Table 2) were then calibrated using three standards (i.e., USGS 40, USGS 62, USGS 64). The standard deviations (SDs) of TOC and  $\delta^{13}C_{org}$  are 0.7% (relative) and 0.06% (absolute), respectively, based on USGS 40 (n = 5).

#### 2.4 Ramped-temperature pyrolysis/oxidation analysis

The integrated ramped-temperature pyrolysis/oxidation (RPO) system utilized here comprises primarily of a carrier gas unit, a programmable pyrolysis furnace and an infrared CO<sub>2</sub> analyzer (Supplementary file Fig. S1). The pyrolysis furnace consists of two insulated furnaces (i.e., the upper and the lower) with thermocouples mounted. A large quartz tube was inserted into the middle chamber of furnaces with catalytic wires (Cu, Pt, Ni) placed in the lower half. During each RPO run, a smaller-sized quartz reactor was packed with an aliquot of sediment containing ~1 mg OC near the bottom end, which was then introduced into the upper half of the large quartz tube. Afterwards, the upper furnace was heated at a constant ramping rate of 5 °C min<sup>-1</sup> from ~ 60 °C to > 1000 °C with steady carrier gas flow rates, whereas the lower furnace was maintained isothermally at 800 °C. The carrier gas flow in the inner quartz tube consists of 27 mL min<sup>-1</sup> helium and 3 mL min<sup>-1</sup> diluted oxygen (5% oxygen). This sub-oxidation mode was consistently adopted in this study to circumvent possible charring during pyrolysis as

illustrated by previous studies (Huang et al., 2023; Stoner et al., 2023; Williams et al., 2014). Further, an additional 5 mL min<sup>-1</sup> pure oxygen was introduced to the interface of two furnaces to completely oxidize vaporized OC fragments downstream. For blank control, quartz tubes were combusted at  $1000 \, ^{\circ}$ C for  $\sim 8h$  prior to RPO analyses. Generally, the precision of the ramping temperature rate was < 0.2%; evolved CO<sub>2</sub> concentrations were calibrated against standard gas containing 2000 ppm CO<sub>2</sub>.

## 2.5 Simulation experiment with addition of calcium chloride

Notably, the residual chloride in sediments may generate chlorine gas under ramping temperatures, which further reacts with catalytic wires, and thus, distorts the authenticity of thermograms (Hemingway et al., 2017b; Huang et al., 2023). This consideration was of no concern to acid rinsing aliquots as the majority of chloride ions were removed after repeated rinses and dilution, whereas considerable amount of chloride in acid fumigation counterparts, especially those dried by oven, surged the risk. To continuously track the performance of catalytic wires, we ran an in-house sample (termed "Irati T2") as the standard, under the same conditions (ramped rate, carrier gas flow rate and O<sub>2</sub> concentration), before and after RPO analysis of those fumigation-treated, oven-dried aliquots. The RPO results of standard samples are presented in the supplementary file (Fig. S2).

To further verify the impact of chlorine gas during RPO analysis, a  $CaCl_2$  addition experiment was carried out with the inhouse standard (Irati T2), by assuming that chlorine gas is generated at elevated temperatures from the decomposition of  $CaCl_2$ , the major chloric constitute in acid fumigated sediments. Specifically, one aliquot of Irati T2 was added with  $\sim 30$  mg  $CaCl_2$  powders, whereas another aliquot of Irati T2 was added with  $\sim 30$  mg  $CaCl_2$  powders, moistened with Milli-Q water, oven dried, and then rinsed three times to remove chloride ions (part of  $Ca^{2+}$  and other cations co-precipitated with OC). The amount of  $CaCl_2$  added ( $\sim 30$  mg) was carefully determined as it represents the median of potential  $CaCl_2$  precipitates in four acid fumigated subsamples ( $\sim 20$  mg to > 100 mg). Subsequently, two aliquots were successively analyzed for RPO and compared with results of raw Irati T2 material.

#### 2.6 Data analysis

120

125

130

135

140

Based on aforementioned experimental design, RPO analyses were conducted for all acidified aliquots and homogenized raw (unacidified) materials. RPO thermograms were further converted to probability density distributions (i.e, p[E]) by the inverse method (Hemingway et al., 2017a), following an open-source package "rampedpyrox" in Python (Hemingway, 2017). Three fundamental parameters, including the mean value of E (termed " $\mu_E$ "), the standard deviation of E (termed " $\sigma_E$ "), and the proportion of OC within a specific range of E (e.g., a kJ mol<sup>-1</sup> to b kJ mol<sup>-1</sup>; termed " $f_{a < E < b}$ "), were calculated for statistic analyses. The default value of the lower bound "a" is 50 kJ mol<sup>-1</sup>, if not specified.

The mean of E was calculated as:

$$145 \quad \mu_E = \int_0^\infty Ep(E)dE \tag{1}$$

The square root of the variance of E was calculated as:

$$\sigma_{\rm F} = (\mu_{\rm F}^2 - [\mu_{\rm F}]^2)^{1/2} \tag{2}$$

The proportion of OC within a specific E range (a kJ mol<sup>-1</sup> to b kJ mol<sup>-1</sup>) was calculated as:

$$f_{a \le E \le b} = \int_a^b p(E) dE \tag{3}$$

RPO parameters measured and/or calculated as well as bulk parameters of all subsamples are listed in Table S2. Based on RPO results of the in-house standard (Irati T2; n=8), the standard deviation (SD) of  $\mu_E$  is 0.50 kJ mol<sup>-1</sup>, and SD of  $\sigma_E$  is 0.18 kJ mol<sup>-1</sup>, denoting excellent reproducibility.

#### 3 Results and discussion

165

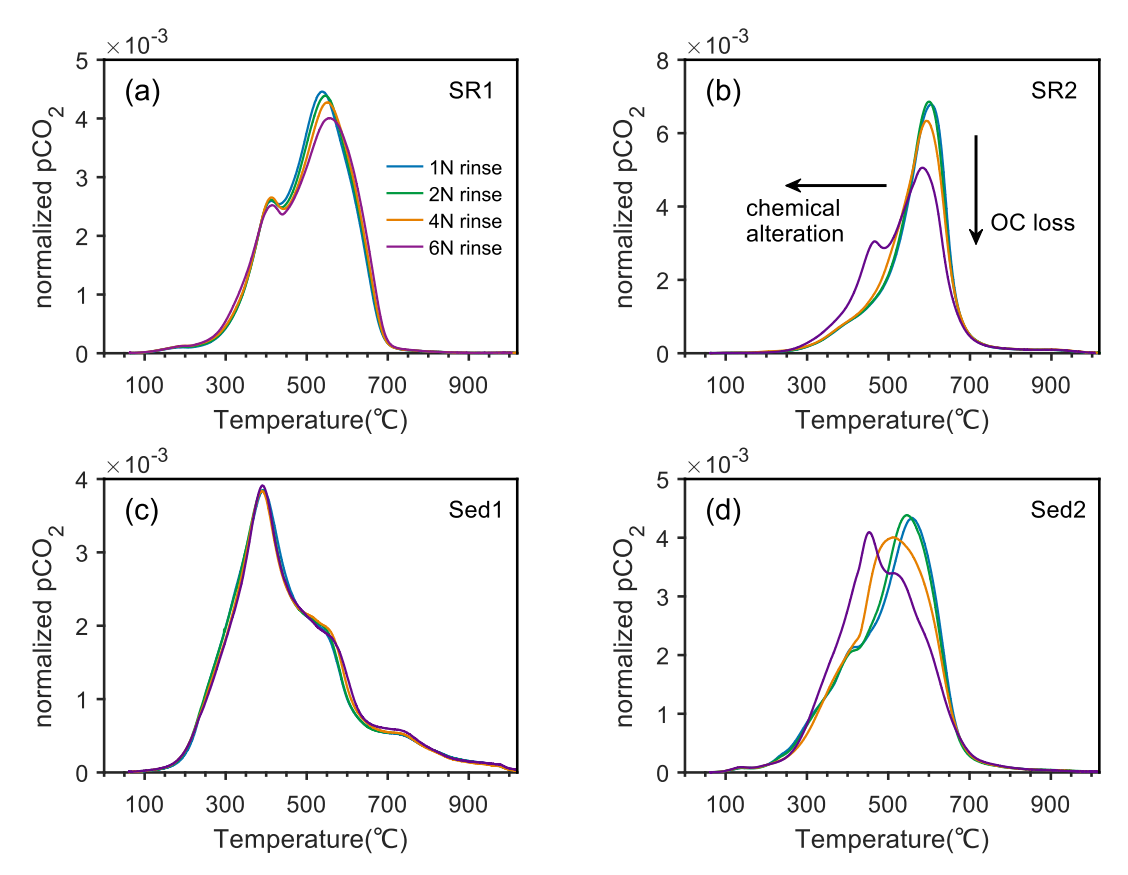
170

#### 3.1 HCl concentration influences on thermochemical properties and potential mechanisms

Ramped-temperature pyrolysis oxidation (RPO) results show that samples after acid rinsing exhibit pronounced deviations in thermograms and energy distributions (Table S2). Although variations of secondary factors (e.g., reaction time, drying methods and temperatures) exert insignificant or erratic influences on the distribution patterns of thermograms (Supplementary file Fig. S3 and S4), thermographic patterns exhibit systematic shifts along the gradient of HCl concentrations (Fig. 1).

To illustrate the inherent consistency between thermograms and HCl concentrations being applied, we orthogonally decomposed evolutionary trends of thermograms into two directions. Changes in the vertical orientation are interpreted as enrichment or loss of OC, whereas horizontal shifts represent alterations in thermal stability and, presumably, structural distortion (Fig. 1). Intriguingly, all four samples in this study exhibit distinct patterns encompassing different vertical and horizontal variations.

Notably, the intensity of OC decomposition at  $T_{max}$  (temperature of maximum CO<sub>2</sub> concentrations) diminishes progressively with increasing HCl concentrations for lithified rock samples (i.e., SR1 and SR2) (Fig. 1a and 1b), consistent with slightly broadening thermograms and elevations in standard deviations of activation energies ( $\sigma_E$ ) (Table S2). Since  $T_{max}$  values are ~ 540 °C and ~ 600 °C for SR1 and SR2, respectively, within the decomposition temperature window of heavily altered petrogenic OC (Hemingway et al., 2018; Venturelli et al., 2020), such decreases in peak CO<sub>2</sub> decomposition also indicate a reduction in the content of thermochemically recalcitrant OC (Bao et al., 2019). In contrary, whereas changes are insignificant in Sed1 (Fig. 1c), a horizontal shift of thermograms towards lower temperatures has been observed for Sed2 (Fig. 1d), suggestive of OC being thermochemically more labile as a consequence of elevated HCl concentrations. With the exception of Sed1, the uniform alteration of OC toward labile thermochemical properties, by lowering proportions of recalcitrant OC and/or shifting thermograms to lower temperatures, implies systematic effects induced by HCl concentrations (Fig. 1).



175 Fig 1: Normalized thermograms of subsamples rinsed with different concentrations of HCl. (a), (b), (c) and (d) are subsamples of SR1, SR2, Sed1 and Sed2, respectively. Two orthogonal arrows in panel (b) indicate different variation modes of thermograms.

180

185

Pronounced variations in thermograms and accordingly enhanced lability of OC under concentrated HCl are likely attributed to structure alteration of mineral matrices and their interactions with OC, in addition to leaching of a fraction of dissolvable OC through acid rinsing. In general, OC exists in sediments in the form of free molecules, aggregates, bound to minerals, or as kerogens. A considerable amount of OC in sediments is stabilized as OC-Fe chelates (Lalonde et al., 2012; Mackey and Zirino, 1994), coated onto mineral surfaces (Mayer, 1994a, b; Vogel et al., 2014), trapped in carbonate matrices (Ingalls et al., 2004; Summons et al., 2013; Yang et al., 2025; Zeller et al., 2020, 2024) and preserved in mineral interlayers (Blattmann et al., 2019; Huang et al., 2023; Kennedy et al., 2002). The dissolution of carbonates under diluted HCl would release OC initially preserved in the carbonate matrix (Zeller et al., 2020), whereas other minerals and OC associated therein are undisturbed. Through carbonate dissolution, a minimal proportion of OC is dissolved in the aqueous phase and washed away at the following water rinsing steps. In comparison, elevated concentrations of HCl would further attack other minerals (e.g., iron oxides, clay minerals) and leach metal ions into solution (Brodie et al., 2011; Fujisaki et al., 2022; Kumar et al., 1995). In fact, former

studies demonstrate that concentrated acids cause metal isotopic fractionations by leaching minerals disproportionally (Fernandez and Borrok, 2009; Rongemaille et al., 2011). Such observation is in consensus with elevated mass loss under concentrated HCl in this study (Table S2). On one hand, concentrated HCl promotes the leaching of OC by releasing and dissolving molecules initially associated with minerals. On the other hand, the destruction of mineral matrix induces profound structural alterations of organic-inorganic complexes (Bao et al., 2019), and reduces organo-mineral binding energy, which is evidenced by shifting E distributions toward lower activation energies (Table S2).

Diverse thermographic shifts along HCl gradients suggest sample-specific impacts of acidification conditions on RPO thermograms and thus warrant careful examination of sample properties. We propose that contrasting variations among samples are primarily driven by organo-mineral interactions and diagenetic alterations. Albeit with contrasting carbonate contents, two lithified sediments respond similarly to elevated HCl concentrations (i.e., denudation in main peak heights and broadening thermograms) without significant thermographic shifts. This is likely due to strong organo-mineral interactions established and homogenized OC properties with time (Craddock et al., 2018; Kennedy et al., 2014). As diagenesis proceeds, processes including the breakdown of biopolymers, modification of functional groups and secondary condensation reactions take place successively (Burdige, 2007), leading to enhanced degrees of reconstruction and lower overall vulnerability to external alterations. In comparison, Sed2 is a modern high-latitude surface sediment with limited diagenetic alteration and hydrodynamic sorting. Accordingly, the majority of OC is likely bound to minerals loosely, and thus would respond considerably to acid concentrations through reversibly breaking or re-establishing weak bonds, which is expressed as horizontal shifts of thermograms (Fig. 1). Conversely, Sed1 represents sediments deposited under aerobic settings on an expansive shelf after extensive degradation along fluvial systems. Consequently, OC preserved therein, regardless of its terrestrial or marine origin, is strongly bond to minerals and thus exhibits sluggish responses to increasing HCl concentrations with nearly overlapping thermograms (Fig. 1) (Huang et al., 2023).

#### 3.2 Thermographic distortion by acid fumigation and the effect of calcium chloride

200

205

210

215

Significant discrepancies are observed in RPO thermograms between acid fumigation and acid rinsing (Fig. 2), as conventional acid fumigation (i.e., without water rinsing) largely lowers or diversifies thermochemical stability of OC. This is related to two putative mechanisms. On one hand, acid fumigation establishes an ambient environment of vaporized HCl, which further attacks sample particles through formation of concentrated HCl solution (Bao et al., 2019). On the other hand, CaCl<sub>2</sub> forms after decarbonation further interacts with OC and alters the structure of OC and organo-mineral interactions during combustion (Wu et al., 2024).

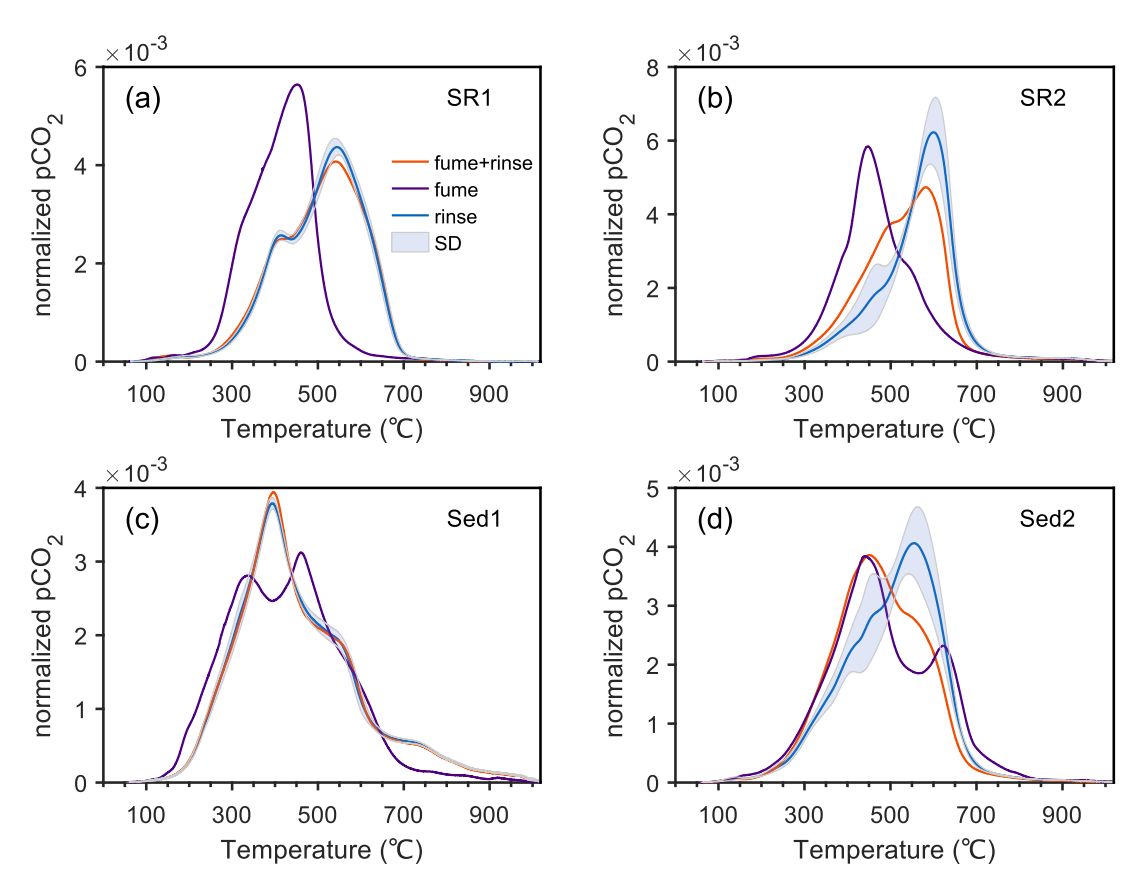


Fig 2: Normalized thermograms of subsamples after acid rinsing and fumigation. (a), (b), (c) and (d) represent subsamples of SR1, SR2, Sed1 and Sed2, respectively. Purple curves and orange curves present subsamples acidified using typical fumigation method and fumigation-rinsing method, while blue curves are mean values of acid rinsed subsamples (Table S1) with shaded intervals representative of standard deviations.

The impact of concentrated HCl generated from acid vapor condensation is assessed through acid fumigation-rinsing experiment (fumigation + rinsing; Table 1). Under this experiment, acid fumigated powders are further rinsed with Milli-Q water to remove HCl and CaCl<sub>2</sub>, which eliminates potential effects of residual HCl and CaCl<sub>2</sub> vapor upon RPO analysis. Results show that thermograms of fumigation-rinsing subsamples are, in general, comparable to those of HCl rinsed subsamples, exhibiting a consistent thermographic shift toward more concentrated HCl conditions (e.g., 12 N HCl) (Fig. 2). Therefore, it indicates that acid fumigation through the condensation of HCl vapor exerts a noticeable and systematic impact on the thermochemical characteristics of sedimentary OC.

225

230 The contrasting results between typical fumigation and fumigation-rinsing methods suggest that CaCl<sub>2</sub> may play an additionally dominant role in modifying thermochemical properties of sedimentary OC, given the residual CaCl<sub>2</sub> being the main difference between these two groups. We propose that CaCl<sub>2</sub> may influence thermograms in two contrary ways. First,

HCl or chlorine gas may boost the breakup of organo-mineral bonds or covalent OC bonds and thus stimulate the decomposition of OC at elevated temperature (Plante et al., 2013). In the meantime, chlorine gas generated through the decomposition of CaCl<sub>2</sub> under high temperatures interacts directly with the catalytic wires (Hemingway et al., 2017b), corrodes reactor tubes (Supplementary file Fig. S5), and thus, influences the thermochemical reaction rates. Conversely, calcium ions (and other metal ions) may enhance organo-cation interactions or facilitate organo-mineral aggregations (Keil and Mayer, 2014; Rowley et al., 2018; Sowers et al., 2018), and thus complicate reaction kinetics. It has been demonstrated that Ca<sup>2+</sup> in soils and sediments enhances the sorption and stabilization of OC (Feng et al., 2005; Rowley et al., 2018). However, the proposed Ca-stabilization mechanism contradicts the observation of fumigated OC being more labile. Therefore, it is possible that HCl and chlorine gas, other than the calcium ion, play a more important role in affecting the ultimate thermochemical decomposition of sedimentary OC after fumigation.

The assumption of thermochemical biases induced by CaCl<sub>2</sub> is further verified by the CaCl<sub>2</sub> addition experiment with the inhouse standard (Irati T2). Consistent with the assumption above, the thermogram of Irati T2 with the addition of CaCl<sub>2</sub> is distinct from those of raw material and CaCl<sub>2</sub> addition-rinsing (Fig. 3). Therefore, it demonstrates that thermographic distortion of fumigated subsamples is most likely an artifact of CaCl<sub>2</sub>. We further measured the raw Irati T2 material before and after the analyses of fumigated subsamples, which apparently corrodes and melts catalytic wires. Invariable thermograms of Irati T2, yet significantly declined CO<sub>2</sub> yield after the analysis of fumigated subsamples suggest insignificant thermographic distortions but incomplete catalytic conversion of CO to CO<sub>2</sub> after the corrosion of the catalytic wires (Fig. S2). Overall, the above results suggest that CaCl<sub>2</sub> biases the thermographic distortion by dictating the pyrolytic breakdown of sedimentary OC.

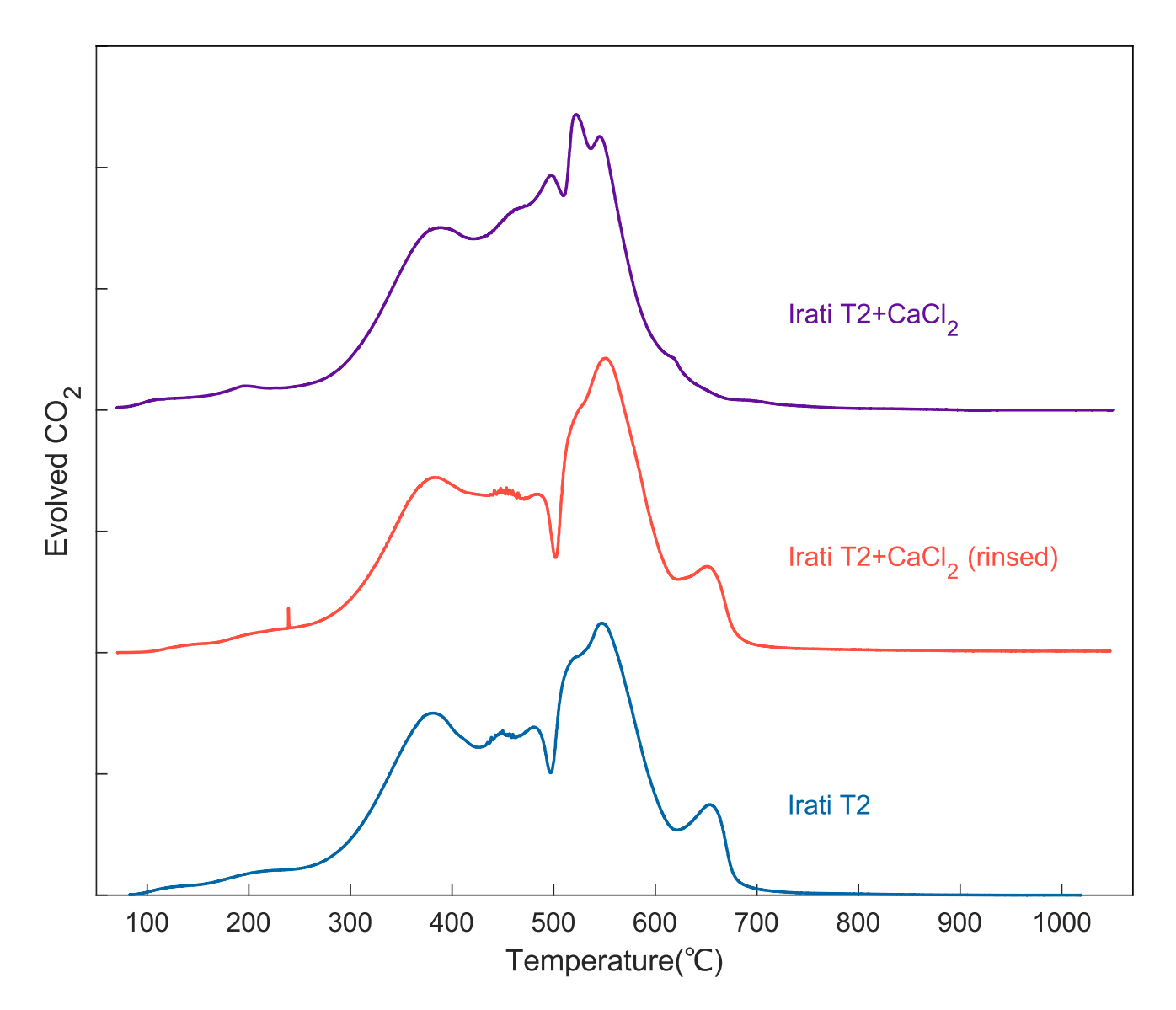


**Fig 3:** Parallel thermograms of the in-house standard (Irati T2) with distinct treatments. From bottom to top, the blue curve is Irati T2 without any extra treatment; the dark orange curve represents Irati T2 mixed with ∼30 mg CaCl₂ and then rinsed with Milli-Q water preceding RPO analysis; the dark purple curve is Irati T2 with addition of ∼30 mg CaCl₂ preceding RPO analysis. All samples were analyzed in sequence within two days to alleviate potential systematic biases with time.

## 3.3 Decarbonation pretreatments deviate thermochemical properties from pristine conditions

260

265

270

Given diverse responses of sediments to HCl concentrations and acid fumigation, it is reasonable to assume that all pretreatment conditions would have resulted in traceable deviation of sample properties away from pristine conditions held by unprocessed raw materials. This is verified and examined by comparing RPO thermograms between acidified (i.e., rinsing, fumigation) and unacidified subsamples. Due to the influence of IC in raw materials, thermograms of both processed and raw sediments were first normalized to back-calculated TOC content of each specific sample. As organic carbon contents of raw subsamples cannot be directly estimated, we used back-calculated TOC of fumigated subsamples, which minimize OC loss, to approximate those of raw subsamples. Former studies suggested that IC decomposition normally commences at  $\sim 500$  °C or higher (Capel et al., 2006; Hemingway et al., 2017a). Thus, we only focus on thermographic segments evolved under 450 °C, below which IC decomposition and consequential CO<sub>2</sub> production are considered to be negligible. Accordingly, we assume that any apparent inconformity of thermograms is ascribed to OC decomposition or alteration.

When thermograms are overlain together, acid rinsed subsamples, with the exception of Sed2, are, on average, more similar to pristine conditions (Fig. 4). It is noteworthy that the instantaneous CO<sub>2</sub> concentrations of raw material may be overestimated, due to the potential decomposition of some carbonate minerals at lower temperatures (Hazra et al., 2022; Sebag et al., 2018) and/or OC loss during acid fumigation. Low-temperature-prone carbonates may reasonably explain the abnormality of Sed2, of which the raw material features relatively low  $\mu_E$  (182.48 kJ mol<sup>-1</sup>; not shown) and  $T_{max}$  value (Supplementary file Fig. S6). Accordingly, we are confident to conclude that acid rinsing is more conducive to maintaining sediment pristine conditions, producing reliable and unbiased thermochemical results.

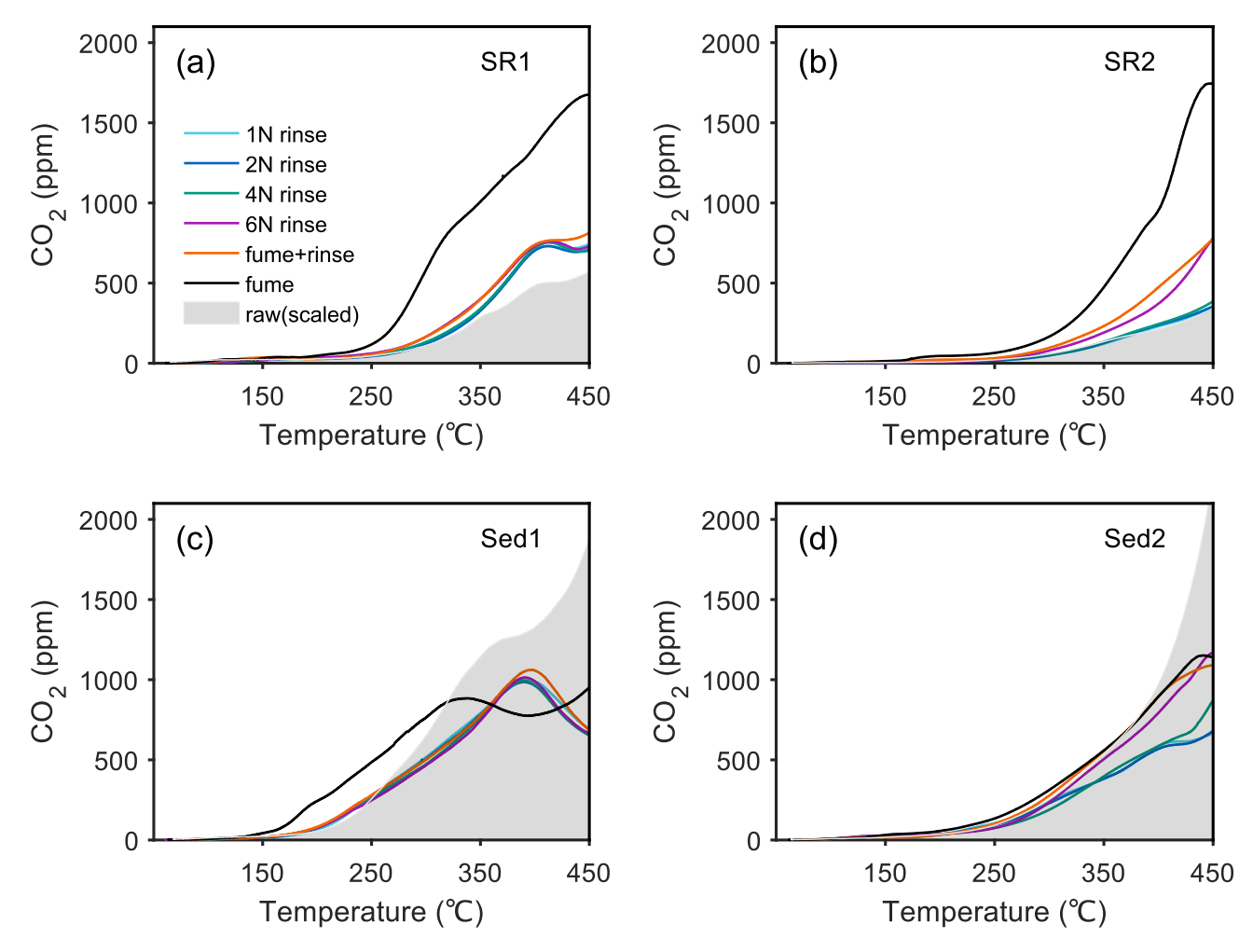


Fig 4: Evaluation of the similarity to the natural pristine states of subsamples acidified by different methods. (a), (b), (c), and (d) are subsamples of SR1, SR2, Sed1, and Sed2, respectively. Each curve represents the thermogram of a subsample acidified by corresponding procedure. The grey area in each subgraph is the thermogram of the raw (unacidified) aliquot after normalization to OC contents.

## 280 4 Conclusion and recommendations

275

285

This study systematically evaluated how decarbonation pretreatments influence ramped-temperature pyrolysis/oxidation (RPO) measurements of sedimentary OC. We demonstrate that both acid rinsing (particularly acid concentration) and fumigation significantly alter thermochemical properties, with higher acid concentrations promoting mineral dissolution, modifying organo-mineral interaction and leaching soluble OC fractions. Crucially, RPO profiles exhibit remarkable methodological differences, where acid fumigation introduces artifacts through corrosive CaCl<sub>2</sub> decomposition and acid vapor exposure, while

acid rinsing with diluted HCl better preserves natural OC characteristics. These findings highlight that pretreatment selection directly impacts the interpretation of thermal degradation characteristics in sedimentary systems.

For reliable RPO analysis, we suggest using diluted HCl rinsing with moderate reaction times (~12h) as the optimal balance between inorganic carbon removal and minimal OC alteration. Other secondary factors (e.g., reaction time) likely have limited impacts on RPO results but may introduce greater biases in bulk carbon measurement. Freeze-drying remains effective but requires strict contamination control (Jiang et al., 2023). While heating accelerates decarbonation, it should be avoided for organic-rich (e.g., protein-rich) sediments to prevent hydrolytic OC loss and leaching of soluble OC. Further studies should incorporate supernatant analysis of acid-soluble OC and complementary techniques like Fourier transform infrared spectroscopy (FTIR) to fully characterize pretreatment impacts (Kleber et al., 2015). Overall, this work establishes that RPO, when paired with appropriate sample preparation, can resolve subtle OC properties obscured by bulk analytical approaches.

## Data availability

290

295

All data needed to evaluate the conclusions is involved in this paper and the supplementary file. The RPO dataset of this study can be accessible through DOI: 10.5281/zenodo.14825000 (He et al., 2025).

## **Author contribution**

300 S.H. and X.C. designed the study; S.H. and H.Y. conducted the experiments; X.C. secured fundings; S.H. drafted the manuscript with contributions from all co-authors.

#### **Competing interests**

The authors declare no conflict of interest.

## Acknowledgements

This work was financially supported by Shanghai "Phosphor" Science Foundation (No. 24QA2704000) and National Natural Science Foundation of China (No. 42273075). We would like to thank Dr. Jordon D. Hemingway for allowing access to the corresponding Python package, Dr. Katarzyna Koziorowska-Makuch for the AREX R7 sample, and Wanhua Huang for the CJK A6-3 sample.

## References

- Bao, R., Strasser, M., McNichol, A. P., Haghipour, N., McIntyre, C., Wefer, G., and Eglinton, T. I.: Tectonically-triggered sediment and carbon export to the Hadal zone, Nat. Commun., 9, 121, https://doi.org/10.1038/s41467-017-02504-1, 2018.
  - Bao, R., McNichol, A. P., Hemingway, J. D., Lardie Gaylord, M. C., and Eglinton, T. I.: Influence of Different Acid Treatments on the Radiocarbon Content Spectrum of Sedimentary Organic Matter Determined by RPO/Accelerator Mass Spectrometry, Radiocarbon, 61, 395–413, https://doi.org/10.1017/RDC.2018.125, 2019.
- Blattmann, T. M., Liu, Z., Zhang, Y., Zhao, Y., Haghipour, N., Montluçon, D. B., Plötze, M., and Eglinton, T. I.: Mineralogical control on the fate of continentally derived organic matter in the ocean, Science, 366, 742–745, https://doi.org/10.1126/science.aax5345, 2019.
- Brodie, C. R., Leng, M. J., Casford, J. S. L., Kendrick, C. P., Lloyd, J. M., Yongqiang, Z., and Bird, M. I.: Evidence for bias in C and N concentrations and δ13C composition of terrestrial and aquatic organic materials due to pre-analysis acid preparation methods, Chem. Geol., 282, 67–83, https://doi.org/10.1016/j.chemgeo.2011.01.007, 2011.
  - Burdige, D. J.: Preservation of Organic Matter in Marine Sediments: Controls, Mechanisms, and an Imbalance in Sediment Organic Carbon Budgets?, Chem. Rev., 107, 467–485, https://doi.org/10.1021/cr050347q, 2007.
- Capel, E. L., De La Rosa Arranz, J. M., González-Vila, F. J., González-Perez, J. A., and Manning, D. A. C.: Elucidation of different forms of organic carbon in marine sediments from the Atlantic coast of Spain using thermal analysis coupled to isotope ratio and quadrupole mass spectrometry, Org. Geochem., 37, 1983–1994, https://doi.org/10.1016/j.orggeochem.2006.07.025, 2006.
  - Craddock, P. R., Bake, K. D., and Pomerantz, A. E.: Chemical, Molecular, and Microstructural Evolution of Kerogen during Thermal Maturation: Case Study from the Woodford Shale of Oklahoma, Energy Fuels, 32, 4859–4872, https://doi.org/10.1021/acs.energyfuels.8b00189, 2018.
- Cui, X., Mucci, A., Bianchi, T. S., He, D., Vaughn, D., Williams, E. K., Wang, C., Smeaton, C., Koziorowska-Makuch, K., Faust, J. C., Plante, A. F., and Rosenheim, B. E.: Global fjords as transitory reservoirs of labile organic carbon modulated by organo-mineral interactions, Sci. Adv., 8, eadd0610, https://doi.org/10.1126/sciadv.add0610, 2022.
- De Lecea, A. M., Smit, A. J., and Fennessy, S. T.: The effects of freeze/thaw periods and drying methods on isotopic and elemental carbon and nitrogen in marine organisms, raising questions on sample preparation, Rapid Commun. Mass Spectrom., 25, 3640–3649, https://doi.org/10.1002/rcm.5265, 2011.
  - Feng, X., Simpson, A. J., and Simpson, M. J.: Chemical and mineralogical controls on humic acid sorption to clay mineral surfaces, Org. Geochem., 36, 1553–1566, https://doi.org/10.1016/j.orggeochem.2005.06.008, 2005.
  - Fernandez, A. and Borrok, D. M.: Fractionation of Cu, Fe, and Zn isotopes during the oxidative weathering of sulfide-rich rocks, Chem. Geol., 264, 1–12, https://doi.org/10.1016/j.chemgeo.2009.01.024, 2009.
- Fujisaki, W., Matsui, Y., Ueda, H., Sawaki, Y., Suzuki, K., and Maruoka, T.: Pre-treatment Methods for Accurate Determination of Total Nitrogen and Organic Carbon Contents and their Stable Isotopic Compositions: Re-evaluation from Geological Reference Materials, Geostand. Geoanalytical Res., 46, 5–19, https://doi.org/10.1111/ggr.12410, 2022.
  - Galy, V., Bouchez, J., and France-Lanord, C.: Determination of Total Organic Carbon Content and  $\delta^{13}$  C in Carbonate-Rich Detrital Sediments, Geostand. Geoanalytical Res., 31, 199–207, https://doi.org/10.1111/j.1751-908X.2007.00864.x, 2007.

- Harris, D., Horwáth, W. R., and Van Kessel, C.: Acid fumigation of soils to remove carbonates prior to total organic carbon or CARBON-13 isotopic analysis, Soil Sci. Soc. Am. J., 65, 1853–1856, https://doi.org/10.2136/sssaj2001.1853, 2001.
  - Hazra, B., Katz, B. J., Singh, D. P., and Singh, P. K.: Impact of siderite on Rock-Eval S3 and oxygen index, Mar. Pet. Geol., 143, 105804, https://doi.org/10.1016/j.marpetgeo.2022.105804, 2022.
- He, S., Yang, H., and Cui, X.: Dataset for acidification impacts on sediment decarbonation (V1.0), https://doi.org/10.5281/ZENODO.14825000, 2025.
  - Hedges, J. I. and Stern, J. H.: Carbon and nitrogen determinations of carbonate-containing solids1, Limnol. Oceanogr., 29, 657–663, https://doi.org/10.4319/lo.1984.29.3.0657, 1984.
  - Hemingway, J. D.: rampedpyrox: Open-source tools for thermoanalytical data analysis, 2016-, https://doi.org/10.5281/zenodo.839815, 2017.
- Hemingway, J. D., Rothman, D. H., Rosengard, S. Z., and Galy, V. V.: Technical note: An inverse method to relate organic carbon reactivity to isotope composition from serial oxidation, Biogeosciences, 14, 5099–5114, https://doi.org/10.5194/bg-14-5099-2017, 2017a.
- Hemingway, J. D., Galy, V. V., Gagnon, A. R., Grant, K. E., Rosengard, S. Z., Soulet, G., Zigah, P. K., and McNichol, A. P.: Assessing the Blank Carbon Contribution, Isotope Mass Balance, and Kinetic Isotope Fractionation of the Ramped Pyrolysis/Oxidation Instrument at NOSAMS, Radiocarbon, 59, 179–193, https://doi.org/10.1017/RDC.2017.3, 2017b.
  - Hemingway, J. D., Hilton, R. G., Hovius, N., Eglinton, T. I., Haghipour, N., Wacker, L., Chen, M.-C., and Galy, V. V.: Microbial oxidation of lithospheric organic carbon in rapidly eroding tropical mountain soils, Science, 360, 209–212, https://doi.org/10.1126/science.aao6463, 2018.
- Hemingway, J. D., Rothman, D. H., Grant, K. E., Rosengard, S. Z., Eglinton, T. I., Derry, L. A., and Galy, V. V.: Mineral protection regulates long-term global preservation of natural organic carbon, Nature, 570, 228–231, https://doi.org/10.1038/s41586-019-1280-6, 2019.
  - Huang, W., Yang, H., He, S., Zhao, B., and Cui, X.: Thermochemical decomposition reveals distinct variability of sedimentary organic carbon reactivity along the Yangtze River estuary-shelf continuum, Mar. Chem., 257, 104326, https://doi.org/10.1016/j.marchem.2023.104326, 2023.
- Ingalls, A. E., Aller, R. C., Lee, C., and Wakeham, S. G.: Organic matter diagenesis in shallow water carbonate sediments, Geochim. Cosmochim. Acta, 68, 4363–4379, https://doi.org/10.1016/j.gca.2004.01.002, 2004.
  - Jiang, C., Robinson, R., Vandenberg, R., Milovic, M., and Neville, L.: Oil contamination of sediments by freeze-drying versus air-drying for organic geochemical analysis, Environ. Geochem. Health, 45, 5799–5811, https://doi.org/10.1007/s10653-023-01594-9, 2023.
- 375 Keil, R. G. and Mayer, L. M.: Mineral Matrices and Organic Matter, in: Treatise on Geochemistry, Elsevier, 337–359, https://doi.org/10.1016/B978-0-08-095975-7.01024-X, 2014.
  - Kennedy, M. J., Pevear, D. R., and Hill, R. J.: Mineral Surface Control of Organic Carbon in Black Shale, Science, 295, 657–660, https://doi.org/10.1126/science.1066611, 2002.

- Kennedy, M. J., Löhr, S. C., Fraser, S. A., and Baruch, E. T.: Direct evidence for organic carbon preservation as clay-organic nanocomposites in a Devonian black shale; from deposition to diagenesis, Earth Planet. Sci. Lett., 388, 59–70, https://doi.org/10.1016/j.epsl.2013.11.044, 2014.
  - Kim, M., Lee, W., Suresh Kumar, K., Shin, K., Robarge, W., Kim, M., and Lee, S. R.: Effects of HCl pretreatment, drying, and storage on the stable isotope ratios of soil and sediment samples, Rapid Commun. Mass Spectrom., 30, 1567–1575, https://doi.org/10.1002/rcm.7600, 2016.
- Kleber, M., Eusterhues, K., Keiluweit, M., Mikutta, C., Mikutta, R., and Nico, P. S.: Mineral–Organic Associations: Formation, Properties, and Relevance in Soil Environments, in: Advances in Agronomy, vol. 130, Elsevier, 1–140, https://doi.org/10.1016/bs.agron.2014.10.005, 2015.
- Komada, T., Anderson, M. R., and Dorfmeier, C. L.: Carbonate removal from coastal sediments for the determination of organic carbon and its isotopic signatures, δ<sup>13</sup> C and Δ<sup>14</sup> C: comparison of fumigation and direct acidification by hydrochloric acid, Limnol, Oceanogr. Methods, 6, 254–262, https://doi.org/10.4319/lom.2008.6.254, 2008.
  - Kumar, P., Jasra, R. V., and Bhat, T. S. G.: Evolution of Porosity and Surface Acidity in Montmorillonite Clay on Acid Activation, Ind. Eng. Chem. Res., 34, 1440–1448, https://doi.org/10.1021/ie00043a053, 1995.
  - Lalonde, K., Mucci, A., Ouellet, A., and Gélinas, Y.: Preservation of organic matter in sediments promoted by iron, Nature, 483, 198–200, https://doi.org/10.1038/nature10855, 2012.
- Lohse, L., Kloosterhuis, R. T., De Stigter, H. C., Helder, W., Van Raaphorst, W., and Van Weering, T. C. E.: Carbonate removal by acidification causes loss of nitrogenous compounds in continental margin sediments, Mar. Chem., 69, 193–201, https://doi.org/10.1016/S0304-4203(99)00105-X, 2000.
  - Mackey, D. J. and Zirino, A.: Comments on trace metal speciation in seawater or do "onions" grow in the sea?, Anal. Chim. Acta, 284, 635–647, https://doi.org/10.1016/0003-2670(94)85068-2, 1994.
- Maier, K. L., Ginnane, C. E., Naeher, S., Turnbull, J. C., Nodder, S. D., Howarth, J., Bury, S. J., Hilton, R. G., and Hillman, J. I.: Earthquake-triggered submarine canyon flushing transfers young terrestrial and marine organic carbon into the deep sea, Earth Planet. Sci. Lett., 654, 119241, https://doi.org/10.1016/j.epsl.2025.119241, 2025.
  - Mayer, L. M.: Relationships between mineral surfaces and organic carbon concentrations in soils and sediments, Chem. Geol., 114, 347–363, https://doi.org/10.1016/0009-2541(94)90063-9, 1994a.
- Mayer, L. M.: Surface area control of organic carbon accumulation in continental shelf sediments, Geochim. Cosmochim. Acta, 58, 1271–1284, https://doi.org/10.1016/0016-7037(94)90381-6, 1994b.
  - McClymont, E. L., Martínez-Garcia, A., and Rosell-Melé, A.: Benefits of freeze-drying sediments for the analysis of total chlorins and alkenone concentrations in marine sediments, Org. Geochem., 38, 1002–1007, https://doi.org/10.1016/j.orggeochem.2007.01.006, 2007.
- Pasquier, V., Sansjofre, P., Lebeau, O., Liorzou, C., and Rabineau, M.: Acid digestion on river influenced shelf sediment organic matter: Carbon and nitrogen contents and isotopic ratios, Rapid Commun. Mass Spectrom., 32, 86–92, https://doi.org/10.1002/rcm.8014, 2018.
  - Plante, A. F., Beaupré, S. R., Roberts, M. L., and Baisden, T.: Distribution of Radiocarbon Ages in Soil Organic Matter by Thermal Fractionation, Radiocarbon, 55, 1077–1083, https://doi.org/10.1017/S0033822200058215, 2013.

- Rongemaille, E., Bayon, G., Pierre, C., Bollinger, C., Chu, N. C., Fouquet, Y., Riboulot, V., and Voisset, M.: Rare earth 415 elements cold seep carbonates from Niger Chem. Geol.. 196-206. in the delta. 286. https://doi.org/10.1016/j.chemgeo.2011.05.001, 2011.
- Rosenheim, B. E., Day, M. B., Domack, E., Schrum, H., Benthien, A., and Hayes, J. M.: Antarctic sediment chronology by programmed-temperature pyrolysis: Methodology and data treatment, Geochem. Geophys. Geosystems, 9, 2007GC001816, https://doi.org/10.1029/2007GC001816, 2008.
  - Rosenheim, B. E., Santoro, J. A., Gunter, M., and Domack, E. W.: Improving Antarctic Sediment<sup>14</sup> C Dating Using Ramped Pyrolysis: An Example from the Hugo Island Trough, Radiocarbon, 55, 115–126, https://doi.org/10.2458/azu js rc.v55i1.16234, 2013.
- Rowley, M. C., Grand, S., and Verrecchia, É. P.: Calcium-mediated stabilisation of soil organic carbon, Biogeochemistry, 137, 27–49, https://doi.org/10.1007/s10533-017-0410-1, 2018.
  - Schlacher, T. A. and Connolly, R. M.: Effects of acid treatment on carbon and nitrogen stable isotope ratios in ecological samples: a review and synthesis, Methods Ecol. Evol., 5, 541–550, https://doi.org/10.1111/2041-210X.12183, 2014.
- Sebag, D., Garcin, Y., Adatte, T., Deschamps, P., Ménot, G., and Verrecchia, E. P.: Correction for the siderite effect on Rock-Eval parameters: Application to the sediments of Lake Barombi (southwest Cameroon), Org. Geochem., 123, 126–135, https://doi.org/10.1016/j.orggeochem.2018.05.010, 2018.
  - Serrano, O., Mazarrasa, I., Fourqurean, J. W., Serrano, E., Baldock, J., and Sanderman, J.: Flaws in the methodologies for organic carbon analysis in seagrass blue carbon soils, Limnol. Oceanogr. Methods, 21, 814–827, https://doi.org/10.1002/lom3.10583, 2023.
- Sowers, T. D., Stuckey, J. W., and Sparks, D. L.: The synergistic effect of calcium on organic carbon sequestration to ferrihydrite, Geochem. Trans., 19, https://doi.org/10.1186/s12932-018-0049-4, 2018.
  - Stoner, S. W., Schrumpf, M., Hoyt, A., Sierra, C. A., Doetterl, S., Galy, V., and Trumbore, S.: How well does ramped thermal oxidation quantify the age distribution of soil carbon? Assessing thermal stability of physically and chemically fractionated soil organic matter, Biogeosciences, 20, 3151–3163, https://doi.org/10.5194/bg-20-3151-2023, 2023.
- Summons, R. E., Bird, L. R., Gillespie, A. L., Pruss, S. B., Roberts, M., and Sessions, A. L.: Lipid biomarkers in ooids from different locations and ages: evidence for a common bacterial flora, Geobiology, 11, 420–436, https://doi.org/10.1111/gbi.12047, 2013.
  - Venturelli, R. A., Siegfried, M. R., Roush, K. A., Li, W., Burnett, J., Zook, R., Fricker, H. A., Priscu, J. C., Leventer, A., and Rosenheim, B. E.: Mid-Holocene Grounding Line Retreat and Readvance at Whillans Ice Stream, West Antarctica, Geophys. Res. Lett., 47, e2020GL088476, https://doi.org/10.1029/2020GL088476, 2020.
- Vogel, C., Mueller, C. W., Höschen, C., Buegger, F., Heister, K., Schulz, S., Schloter, M., and Kögel-Knabner, I.: Submicron structures provide preferential spots for carbon and nitrogen sequestration in soils, Nat. Commun., 5, 2947, https://doi.org/10.1038/ncomms3947, 2014.
- Williams, E. K., Rosenheim, B. E., McNichol, A. P., and Masiello, C. A.: Charring and non-additive chemical reactions during ramped pyrolysis: Applications to the characterization of sedimentary and soil organic material, Org. Geochem., 77, 106–114, https://doi.org/10.1016/j.orggeochem.2014.10.006, 2014.

- Wu, Y., Zhang, Q., Zhuo, J., Dong, S., and Yao, Q.: Influence of calcium chloride on the fine particulate matter formation during coal pyrolysis, Fuel, 355, 129480, https://doi.org/10.1016/j.fuel.2023.129480, 2024.
- Yamamuro, M. and Kayanne, H.: Rapid direct determination of organic carbon and nitrogen in carbonate-bearing sediments with a Yanaco MT-5 CHN analyzer, Limnol. Oceanogr., 40, 1001–1005, https://doi.org/10.4319/lo.1995.40.5.1001, 1995.
- 455 Yang, H., Ma, J., He, S., Wang, J., Sun, Y., and Cui, X.: Resistant degradation of petrogenic organic carbon in the weathering of calcareous rocks, Glob. Planet. Change, 246, 104727, https://doi.org/10.1016/j.gloplacha.2025.104727, 2025.
  - Zeller, M. A., Van Dam, B. R., Lopes, C., and Kominoski, J. S.: Carbonate-Associated Organic Matter Is a Detectable Dissolved Organic Matter Source in a Subtropical Seagrass Meadow, Front. Mar. Sci., 7, 580284, https://doi.org/10.3389/fmars.2020.580284, 2020.
- Zeller, M. A., Van Dam, B. R., Lopes, C., McKenna, A. M., Osburn, C. L., Fourqurean, J. W., Kominoski, J. S., and Böttcher, M. E.: The unique biogeochemical role of carbonate-associated organic matter in a subtropical seagrass meadow, Commun. Earth Environ., 5, 681, https://doi.org/10.1038/s43247-024-01832-7, 2024.
- Zhang, X., Bianchi, T. S., Cui, X., Rosenheim, B. E., Ping, C., Hanna, A. J. M., Kanevskiy, M., Schreiner, K. M., and Allison, M. A.: Permafrost Organic Carbon Mobilization From the Watershed to the Colville River Delta: Evidence From<sup>14</sup> C Ramped Pyrolysis and Lignin Biomarkers, Geophys. Res. Lett., 44, https://doi.org/10.1002/2017GL075543, 2017.
  - Zhang, Y., Galy, V., Yu, M., Zhang, H., and Zhao, M.: Terrestrial organic carbon age and reactivity in the Yellow River fueling efficient preservation in marine sediments, Earth Planet. Sci. Lett., 585, 117515, https://doi.org/10.1016/j.epsl.2022.117515, 2022.